REPORT DOCUMENTATION PAGE

Form Approved
OMB No. 0704-0188

1. REPORT DATE *(DD-MM-YYYY)*	**2. REPORT TYPE**	**3. DATES COVERED** *(From - To)*
2013	Open Literature	

4. TITLE AND SUBTITLE
Evaluation and computational characterization of the facilitated transport of Glc carbon C-1 oxime reactivators across a blood brain barrier model

5a. CONTRACT NUMBER

5b. GRANT NUMBER
1.E005.08.WR

5c. PROGRAM ELEMENT NUMBER

6. AUTHOR(S)
Bhonsle, JB, Causey, R, Oyler, BL, Bartochucci, C, Lamba, D, Pesaresi, A, Bhamare, NK,

5d. PROJECT NUMBER

5e. TASK NUMBER

5f. WORK UNIT NUMBER

7. PERFORMING ORGANIZATION NAME(S) AND ADDRESS(ES)

US Army Medical Research Institute of Chemical Defense
ATTN: MCMR-CDR-I
3100 Ricketts Point Road
Aberdeen Proving Ground, MD
21010-5400

8. PERFORMING ORGANIZATION REPORT NUMBER

USAMRICD-P12-025

9. SPONSORING / MONITORING AGENCY NAME(S) AND ADDRESS(ES)
Defense Threat Reduction Agency
8725 John J. Kingman Road STOP 6201
Fort Belvoir, VA 22060-6201

10. SPONSOR/MONITOR'S ACRONYM(S)

11. SPONSOR/MONITOR'S REPORT NUMBER(S)

12. DISTRIBUTION / AVAILABILITY STATEMENT

Approved for public release; distribution unlimited

13. SUPPLEMENTARY NOTES
Published in Chemico-Biological Interactions 203 (2013) 129–134. This work was supported by Defense Threat Reduction Agency (Grant number 1.E005.08.WR).

14. ABSTRACT
See reprint.

15. SUBJECT TERMS
Facilitated transport, Sugar-oximes, Sox, Blood brain barrier, Reactivation, Acetylcholinesterase

16. SECURITY CLASSIFICATION OF:			**17. LIMITATION OF ABSTRACT**	**18. NUMBER OF PAGES**	**19a. NAME OF RESPONSIBLE PERSON**
a. REPORT	**b. ABSTRACT**	**c. THIS PAGE**			Gregory Garcia
UNCLASSIFIED	UNCLASSIFIED	UNCLASSIFIED	UNLIMITED	6	**19b. TELEPHONE NUMBER** *(include area code)* 410-436-6009

Chemico-Biological Interactions 203 (2013) 129–134

Contents lists available at SciVerse ScienceDirect

Chemico-Biological Interactions

journal homepage: www.elsevier.com/locate/chembioint

Evaluation and computational characterization of the facilitated transport of Glc carbon C-1 oxime reactivators across a blood brain barrier model

Jayendra B. Bhonsle [a], Robert Causey [b], Benjamin L. Oyler [c], Cecilia Bartolucci [d], Doriano Lamba [e], Alessandro Pesaresi [e], Nanaji K. Bhamare [b], Iswarduth Soojhawon [f], Gregory E. Garcia [b,*]

[a] Astha Drug Discovery & Research, 5284 Randolph Road #262, Rockville, MD 20852, USA
[b] Research Division, US Army Medical Research Institute of Chemical Defense, 3100 Ricketts, Point Road, Aberdeen Proving Ground, MD 21010-5400, USA
[c] Analytical Toxicology Division, US Army Medical Research Institute of Chemical Defense, 3100 Ricketts Point Road, Aberdeen Proving Ground, MD 21010-5400, USA
[d] Istituto di Cristallografia, Consiglio Nazionale delle Ricerche, Area della Ricerca di Roma, Via Salaria Km. 29.300, I-00015 Monterotondo Scalo, Roma, Italy
[e] Istituto di Cristallografia, Consiglio Nazionale delle Ricerche, Area Science Park, Basovizza, S.S. 14, Km. 163.5, I-34149 Trieste, Italy
[f] Division of Biochemistry, Walter Reed Army Institute of Research, 503 Robert Grant Road, Silver Spring, MD 20910-7500, USA

ARTICLE INFO

Article history:
Available online 13 October 2012

Keywords:
Facilitated transport
Sugar-oximes
SOx
Blood brain barrier
Reactivation
Acetylcholinesterase

ABSTRACT

We are evaluating a facilitative transport strategy to move oximes across the blood brain barrier (BBB) to reactivate inhibited brain acetylcholinesterase (AChE). We selected glucose (Glc) transporters (GLUT) for this purpose as these transporters are highly represented in the BBB. Glc conjugates have successfully moved drugs across the BBB and previous work has shown that Glc-oximes (sugar-oximes, SOxs) can reduce the organophosphonate induced hypothermia response. We previously evaluated the reactivation potential of Glc carbon C-1 SOxs. Here we report the reactivation parameters for VX- and GB-inhibited human (Hu) AChE of the best SOx (**13c**) and our findings that the kinetics are similar to those of the parent oxime. Although crystals of *Torpedo californica* AChE were produced, neither soaked or co-crystallized experiments were successful at concentrations below 20 mM **13c**, and higher concentrations cracked the crystals. **13c** was non-toxic to neuroblastoma and kidney cell lines at 12–18 mM, allowing high concentrations to be used in a BBB kidney cell model. The transfer of **13c** from the donor side was asymmetric with the greatest loss of **13c** from the apical- or luminal-treated side. There was no apparent transfer from the basolateral side. The **13c** P_{app} results indicate a 'low' transport efficiency; however, mass accounting revealed only a 20% recovery from the apical dose in which high concentrations were found in the cell lysate fraction. Molecular modeling of **13c** through the GLUT-1 channel demonstrated that transport of **13c** was more restricted than Glc. Selected sites were compared and the **13c** binding energies were greater than two times those of Glc.

Published by Elsevier Ireland Ltd.

1. Introduction

Currently fielded oxime reactivators 2-pralidoxime (2-PAM), obidoxime and potential replacements 1,1′-methylenebis[4-[(hydroxyimino)methyl]-pyridinium] dimethanesulfonate (MMB-4) and [(*E*)-[1-[(4-carbamoylpyridin-1-ium-1-yl)methoxymethyl]pyridin-2-ylidene]methyl]-oxoazaniumdichloride (HI-6), do not appreciably cross the blood brain barrier (BBB) and do not prevent OP-induced brain seizure activity [1–3]. The BBB is comprised of an endothelial cell layer with tighter intercellular junctions as compared to normal capillaries [4]. BBB-penetrating oximes such as monoisonitrosoacetone (MINA) and dihydropyridine 2-pralidoxime (pro-2-PAM) can act centrally and abrogate brain OP-induced seizure activity [5,6], but these compounds or their breakdown products may be too toxic for use [6,7]. Other strategies to deliver oximes across the BBB (reviewed by Mercey et al. [8]) include facilitative transport where sugar-oxime (SOx) conjugates could be transferred by glucose (Glc) transporters (GLUT) [9]. GLUTs are abundant in the BBB with GLUT-1 capillary density of 80–90 pmol/mg membranes [10]. Glc-conjugate transport has been reported [11–13]. GLUTs have not yet been crystallized, but a homology model based upon the bacterial glycerol-3-phosphate transporter (PDB ID 1PW4 [14]) was developed and reported by Salas-Burgos et al. (PDB ID 1SUK [15]) and formed the basis for studies to explore Glc transporters as a facilitative transport mechanism to improve reactivator penetration across the BBB.

Expanding on the work of Heldman et al. [16] we compared their best SOx (N-[(3-β-D-glucopyranosyloxy)propyl]-4-pyridiniumaldoxime chloride (**8b**)) and a novel SOx of our own design [9] (Fig. 1). Our SOx, N-[(3-β-D-glucopyranosyloxy)octyl]-2-pyridiniumaldoxime iodide (**13c**), reactivated 133% and 113% better than **8b** for diisopropylfluorophosphate- and paraoxon-inhibited

* Corresponding author. Tel.: +1 410 436 6009; fax: +1 410 436 8377.
E-mail address: Gregory.E.Garcia@us.army.mil (G.E. Garcia).

0009-2797/$ - see front matter Published by Elsevier Ireland Ltd.
http://dx.doi.org/10.1016/j.cbi.2012.09.012

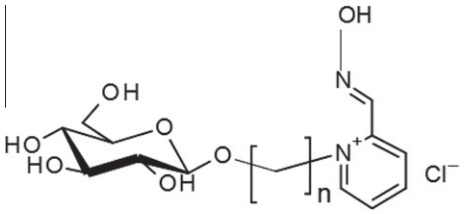

Fig. 1. Structures for Glc-1-position ether sugar-oxime series of compounds. Specific compounds (n, parent oxime): **8b** (3, 4PAM); **8c** (3, 2-PAM); **13c** (7,2-PAM).

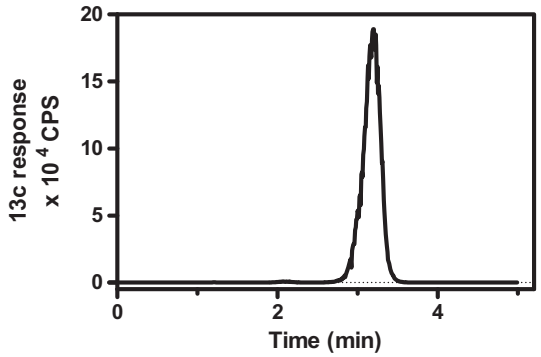

Fig. 2. Multiple reaction monitoring (MRM) chromatogram of **13c** in cell lysate sample from 18 mM apical side treated MDCK BBB model test. **13c** Retention Time = 3.20 min. The transition monitored was 413 → 251 *m/z*. The concentration determined from this test was 175 μM as shown in Table 3.

human red blood cell (Hu RBC) AChE, and we generated pharmacophore models from quantitative structure–activity relationships, and 2D and 3D comparative molecular field analysis models [17]. The pharmacophore computation adjusted (PCA) predicted activity for **13c** had an excellent correlation with the observed activity. We have continued this work and now report the reactivation parameters of these SOxs and the analysis of an additional novel SOx N-[(3-β-D-glucopyranosyloxy)propyl]-2-pyridiniumaldoxime chloride (**8c)** predicted to be active. To gain insights of important molecular contacts between SOx and AChE we explored X-ray crystallographic studies of **8b** and **13c**. In addition, we developed computational models to predict the transport potential of GLUT-1 for novel compounds that could be extremely valuable for designing BBB-penetrating SOxs and correlate this model with experimental results.

2. Materials and methods

2.1. Sugar-oxime synthesis

Materials and reagents were purchased from Sigma–Aldrich (St. Louis, MO). **8c** was synthesized as described earlier [9]. Structures were confirmed by NMR utilizing a Varian Unity INOVA at 600 MHz using 5 mm Penta (H,C,N,P,D) pulse field Z-gradient (PFG) probe at 25 °C and liquid chromatography–mass spectroscopy (LC–MS) (data not shown).

2.2. Reactivation

Human whole blood was obtained from volunteers in accordance with the USAMRICD donor program (USAMRICD M-10088). Hu RBCs were treated with OPs to yield 80–95% inhibited AChE [9]. AChE reactivation was determined at several SOx concentrations and assayed by the discontinuous method [18] to determine the initial (v_i), final (v_0), and intermediate (v_t) AChE activity levels. The data were plotted according to equation $\ln((v_0 - v_t)/(v_0 - v_i)) = -k_{obs}t$ where k_{obs} is estimated as the slope of the best-fit line. A secondary plot was made of k_{obs} vs. [SOx]. The equation $k_{obs} = k_r = SOx/(K_D + SOx)$ and nonlinear regression was used to estimate K_D and k_r. The specific reactivity, k_{r2}, was calculated using equation $k_{r2} = k_r/K_D$. Curve fitting was done using Prism software Ver. 4.0 (Graphpad Inc.).

2.3. Toxicity

Neuroblastoma SHSY-5Y cells were treated with increasing concentrations (0.1–12 mM) of **13c**. The 24 h post-treatment viability was determined using the AqueousOne Cell Titer kit (Promega Corp., Madison, WI).

2.4. Blood brain barrier (BBB) modeling

The multidrug resistance-1 Madin-Darby canine kidney (MDR1-MDCK) cell model was used (Absorptive Systems Inc., Exton, PA). Compounds were prepared in water. 2-PAM (poor BBB penetrant) was used at 5 μM, and the test compound **13c** was used at 5, 50 μM and 6, 12, and 18 mM. Samples were collected after 2 h. For the mM oxime tests cell lysates were prepared. Lucifer yellow and trans epithelial electric resistance (TEER) measurements were used as culture integrity checks. TEER values ranged from 1640 to 1942 Ohm-cm^2. The apparent permeabilites, P_{app}, were calculated according to Wang et al. [19] for the receiver compartments following apical and basolateral treatment. In these cultures, apical refers to the luminal or exterior side and basolateral refers to the abluminal or tissue compartment side. The brain penetration potential of a test compound is classified as low, moderate, or high using the following criteria: a. Low: P_{app} $A \rightarrow B < 3.0 \times 10^{-6}$ cm/s, b. Low: P_{app} $A \rightarrow B \geqslant 3.0 \times 10^{-6}$ cm/s, Efflux $\geqslant 10$, c. Moderate: P_{app} $A \rightarrow B \geqslant 3.0 \times 10^{-6}$ cm/s, $10 >$ Efflux $\geqslant 3.0$, d. High: P_{app} $A \rightarrow B \geqslant 3.0 \times 10^{-6}$ cm/s, Efflux < 3.0.

2.5. Analytical SOx assay

We developed a more sensitive LC–MS/MS assay than the Creasey and Green assay [20] to analyze blood brain barrier (BBB) samples. Samples were acidified to pH 2 and then deproteinized by ultrafiltration. Samples were stored at −80 °C until use. LC separation was performed using a 1260 series binary pump equipped with a 1290 series autosampler (Agilent, Santa Clara, CA) operated at a flow rate of 300 μL min^{-1} isocratic conditions (44% Solvent A: acetonitrile, 56% Solvent B: 40 mM ammonium acetate) at 24 °C. Separations were over a PolyCAT A column (100 mm × 2.1 mm i.d., 3 μm) and a Javelin (10 mm × 2.1 mm) guard cartridge (PolyLC Inc., Columbia, MD) of 5 μL injections. Oximes were detected with a 4000 QTrap mass spectrometer (AB Sciex, Foster City, CA) equipped with an electrospray ion source operated in positive ionization mode at 5 kV. The source conditions were curtain gas flow of 20 psi, temperature of 50 °C, GS1 (cone gas) at 60 psi, GS2 (desolvation gas) at 25 psi, and interface heater on. Collision gas (nitrogen) was set on "high". Multiple reaction monitoring (MRM) mode was used, and the conditions for each MRM transition were optimized and are as follows:

Transition name	Q1 *m/z*	Q3 *m/z*	Dwell time (ms)	DP	EP	CE	CXP
13c Quantifier	413.3	251.2	150	193.5	7.5	35.09	15.91
13c Qualifier	413.3	122.9	150	193.5	7.5	43.07	6.2
2-PAM	137.1	93.1	150	60.29	13.18	31.12	7.58

DP = declustering potential, EP = entrance potential, CE = collision energy, CXP = collision cell exit potential; all potentials are reported in V.

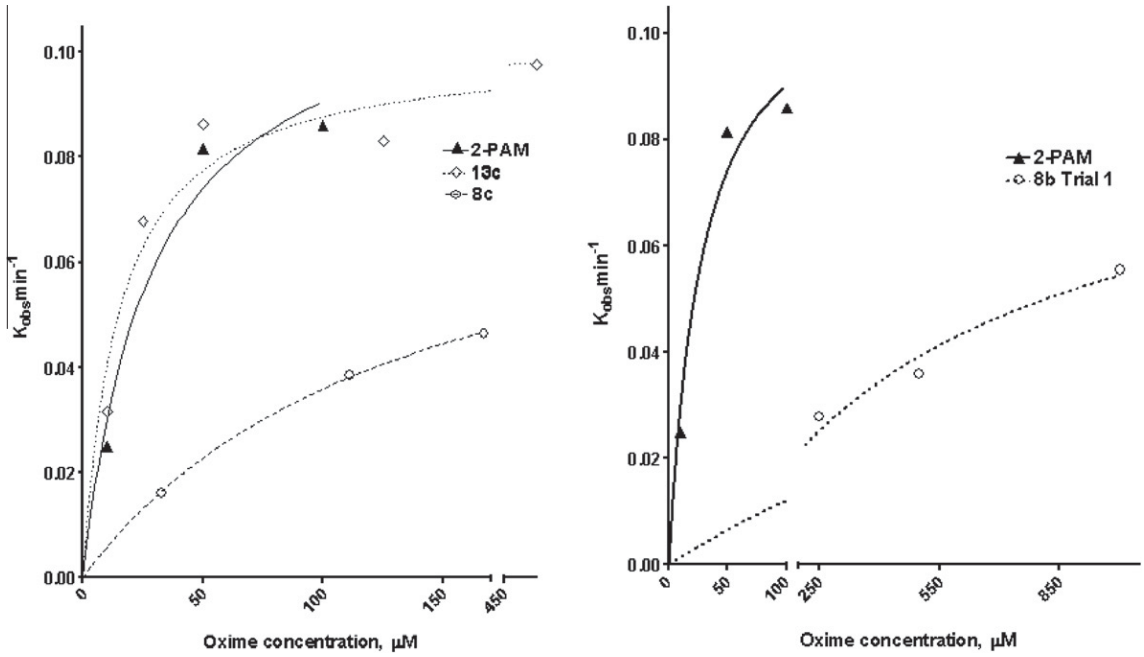

Fig. 3. Reactivation of VX-inhibited hu RBC AChE by 2-PAM and **13c**, **8c** on the left, and **8b** on the right.

Data were processed using Analyst version 1.5.2 (AB Sciex, Foster City, CA). The lower limit of quantitation (LLOQ) for **13c** and 2-PAM was ~20 ng/mL and there was negligible ion-suppression. A LC-MS/MS representative chromatogram from a cell lysate analysis is shown in Fig. 2. Matrix-matched standards were used for standard curve generation.

2.6. Molecular modeling

The translocation of Glc and **13c** through the GLUT-1 receptor was studied using two computational techniques, viz, molecular dynamics (MD) simulation and Glc–GLUT-1 docking studies. The MD simulations were performed using Discovery Studio version 3.1 (DS3.1) molecular modeling software, and the docking studies were performed with Sybyl-X version 1.3 molecular modeling software. All MD simulations with DS3.1 used CHARMm forcefield, Momany–Rone charges and implicit water solvation (Generalized Born approach). All docking studies used Amber7 FF02 force field with Amber charges. PDB ID 1SUK (homology modeling derived structure) was cleaned, solvated in water, and equilibrated while constraining the backbone atoms to preserve the bioactive conformation and optimal side-chain locations. The FlexiDock algorithm based on Genetic algorithm was used for docking. Compounds were positioned manually at the various locations in the Glc channel. Flexidock experiments were performed with the specified number of generations as shown in Table 6. For **13c** docking experiments **13c** was aligned with Glc from the Glc–GLUT1 docked poses. For all MD experiments the standard dynamics cascade protocol as devised in DS3.1 was used. The GLUT-1 backbone atoms were constrained by employing the Fixed Atom constraints method. In the standard dynamics cascade protocol, the NVT approach was employed with the following settings in the minimization (steepest descent 500 steps followed by conjugate descent 500 steps), heating and equilibration (5000 steps each) and production (10,000 steps) steps. The target temperature was set to 310 K to reflect the physiological temperature rather than the standard room temperature.

Table 1
Reactivation parameters of sugar-oximes.

Agent	Oxime	k_r (min)	K_D (μM)	k_{r2} ($min^{-1}mM^{-1}$)	k_{r2} ratio 2-PAM
VX	2-PAM	0.116	28.67	4.060	1.000
	8b	0.089	629	0.141	0.035
	8c	0.085	138.5	0.616	0.152
	13c	0.101	15.08	6.680	1.645
GB	2-PAM	0.131	23.59	5.556	1.000
	8b	0.447	2669	0.168	0.030
	8c	0.063	156.60	0.401	0.072
	13c	0.056	15.45	3.637	0.654

Table 2
SOx **13c** transport in MD-MDCK.

Sample	SOx Concentration		
	Treatment SOx (mM)	Measured SOx (μM)	
	mM	Mean	SD
Apical			
Receiver	6	2.65	0.09
	12	3.56	0.51
	18	7.08	0.22
Cell	6	37.8	6.51
	12	66.1	4.79
	18	175.4	4.28
Donor	6	1169	53.0
	12	2153	283.5
	18	3722	234.2
Basolateral			
Receiver	6	0.82	0.02
	12	1.46	0.29
	18	1.71	0.17
Cell	6	0.77	0.1
	12	1.93	1.04
	18	3.15	0.62
Donor	6	6041	247
	12	11883	135
	18	19554	135

Table 3
List of amino acids involved in the PDB structure 1SUK-defined helices of GLUT-1.

1SUK PDB helices #/amino acid residue #					
PDB-H#	Residue #	PDB-H #	Residue #	PDB-H #	Residue #
H1	S5-G31	H8	L169-N182	H15	N360-F375
H2	I33-I40	H9	L185-P187	H16	V376-F379
H3	T47-R51	H10	L188-C207	H17	G384-A392
H4	T60-F90	H11	R253-E261	H18	L394-N397
H5	G91-S113	H12	R264-Y292	H19	G398-F422
H6	M121-S148	H13	N304-R330	H20	G430-G471
H7	A151-L169	H14	T335-L357	H21	H484-S490

Table 4
List of amino acids involved in the Mueckler defined helices of GLUT-1.

Mueckler 2008 helices #/amino acid residue #					
M-H#	Residue #	M-H#	Residue #	M-H#	Residue #
MH1	S5-I40	MH5	A151-N182	MH9	T335-L357
MH2	T60-F90	MH6	L185-C207	MH10	N360-A392
MH3	G91-S113	MH7	R264-Y292	MH11	L394-F422
MH4	M121-S148	MH8	N304-R330	MH12	G430-G471

Table 5
List of amino acids involved in the GLUT-1 Glucose channel along with the Mueckler and PDB defined helices numbers.

Mueckler helices/PDB helices/amino acid residue #					
M-H#	PDB-H #	Residue #	M−H #	PDB-H #	Residue #
MH1	H2	S23-I40	MH7	H12	R264-Y292
MH2	H4	T60-F90	MH8	H13	N304-R330
MH4	H6	M121-S148	MH10	H15-H18	N360-N397
MH5	H7-H8	A151-N182	MH11	H19-H20	G398-G471

3. Results

3.1. Reactivation

The reactivation of VX-inhibited Hu RBC AChE by 2-PAM and SOxs is shown in Fig. 3 (GB data not shown). The reactivation parameters are shown in Table 1. The k_{r2} ratio of **13c** to 2-PAM was 1.67, while **8c** yielded 0.152 and **8b** 0.035. This indicates that **13c** is the best SOx reactivator to date and that a 2-PAM derivative is better for VX and GB than the 4-PAM derivative. We have previously reported that **13c** is a better reactivator than **13a** (3-PAM derivative) and **13b** (4-PAM derivative) [9], so it appears the preferred parent oxime is 2-PAM.

3.2. Toxicity

13c was found to be nontoxic up to 12 mM (highest concentration tested) for the neuroblastoma cell line SHSY-5Y. **13c** was also well tolerated by MDR1-MDCK cells treated for 2 h in low Glc media (5 mM) with **13c** concentrations as high as 18 mM (the highest concentration tested-data not shown). These results indicate that toxicity of **13c** appears similar to that of **8b** [17].

3.3. Blood brain barrier model

The MDR1-MDCK cell line is a well documented BBB model [20]. This cell line expresses several GLUTs (GLUT-1, 2, 3 and 5) with asymmetric distribution [21]. The P_{app} was low for 5–50 μM concentrations of 2-PAM and **13c** (data not shown). As these experiments were performed in Glc concentrations of 15–20 mM (typical culture media) the experiments were repeated at the physiologically relevant Glc concentration of 5 mM. **13c** concentrations up to 18 mM revealed a dose-dependent asymmetric transference with the apical treatment yielding higher levels in the receiver well and cell lysates. The **13c** P_{app} was low for all concentrations tested with the apical treatment yielding > 4 × the receiver side concentration than the basolateral side as shown in Table 2. The summation of compartment concentrations reveals that 18 mM apical dosing is 20% of that from the basolateral side ((3904.48 μM/19558.86 μM) ∗ 100).

3.4. Modeling

The homology model structure of GLUT-1 (PDB ID 1SUK) was defined to comprise 21 alpha-helices by Salas-Burgos et al. [15], and the amino acids comprising the helices are shown in Table 3. The amino acids comprising the 12 alpha-helices defined by Meuckler et al. [22] are shown in Table 4, which also shows that the Glc channel is flanked by helices 1, 2, 4, 5, 7, 8, 10 and 11. In the PDB 1SUK structure the same Glc channel translates to helices numbering 2, 4, 6, 7, 8, 12, 13, 15, 16, 17, 18, 19 and 20. The exact amino acids defining the Glc channel of the Meuckler et al. helices and PDB 1SUK helices are shown in Table 5. The exact amino acids from the Glc translocation channel have been identified as Glu-254 and Lys-256 [23], Trp-388 [15], and Trp-412 [24]. Seven docking locations in the Glc channel were identified and are listed in Table 6 and named according to their positions in the channel. The outermost docking location is termed extra cellular mouth-1 (ECM-1). The next location, deeper into the mouth, is ECM-2, while the deepest location is ECM-3. The docking location closest to Trp-412 in the central region is termed central Glc channel-1 (CGC-1), and the next location deeper toward the cytoplasm is CGC-2, while the deepest is CGC-3. The docking location at the intra cellular mouth is termed ICM. A GLUT-1 ribbon model is shown in Fig. 4A, and the movement of Glc is shown for the individual sites in Fig. 4B. The docking parameters and results are shown in Table 6. The binding energies of Glc and **13c** varied from −477 to −166 Kcals/mol, and −868 to −269 Kcals/mol, respectively. For both there was a maximum affinity at ECM-2. MD simulations with Glc and **13c** placed at the various positions for time periods of 2 ps

Table 6
Docking experiments parameters and results for Glc and **13c.**

Glc location	Reported Glc binding AA	Binding site # bonds for Glc	FlexiDock # generations for Glc	Obsd binding energy Kcals/mol for Glc	GLUT-1 overlay 1SUK RMSD for Glc	Binding site # bonds for **13c**	FlexiDock # generations for **13c**	Obsd binding energy Kcals/mol for **13c**
ECM-1	–	91	110500	−241.7	0.25	339	181000	−581.9
ECM-2	–	232	122000	−476.7	0.28	444	240000	−867.5
ECM-3	W412	199	105500	−382.8	0.27	487	240000	−750.9
CGC-1	W412	187	122000	−334.7	0.34	453	238000	−743.2
CGC-2	–	112	122000	−166.0	0.27	220	240000	−288.9
CGC-3	W388	107	122000	−168.4	0.27	254	240000	−395.9
ICM	E254/K256	137	122000	−288.6	0.23	137	80000	−268.5

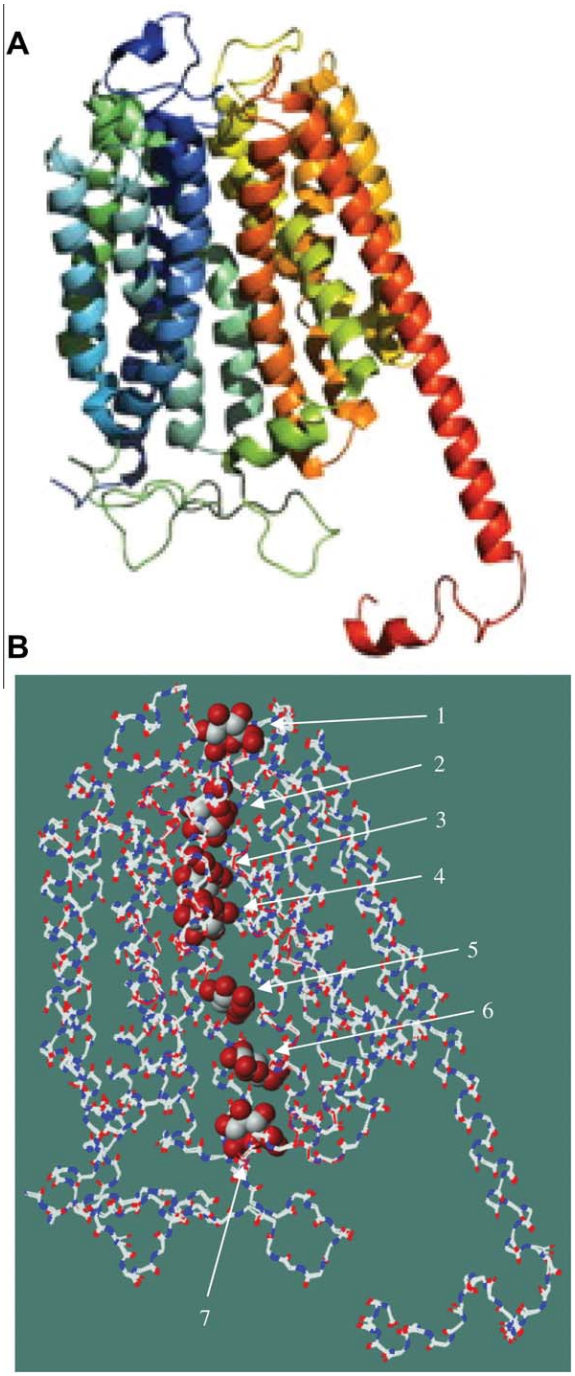

Fig. 4. GLUT-1 structure and Glc movement through channel. (A) Cartoon representation of the GLUT-1 theoretical model (PDB ID 1SUK) [15] created using PyMOL [27]; (B) Picture of binding locations along the Glc channel in GLUT-1 shown with Glc: (1) extra cellular mouth-1 (ECM-1); deeper into the mouth, is (2) ECM-2; deepest location is (3) ECM-3; the docking location closest to Trp-412 in the central region is (4) central Glc channel-1 (CGC-1); next location deeper toward the cytoplasm is (5) CGC-2; the deepest location is (6) CGC-3. The docking location at the intra cellular mouth (ICM) is (7).

showed them traveling in the intracellular mouth direction (data not shown).

4. Discussion

SOxs have now been shown by us and others to be relatively good reactivators compared to monoamine quaternary pralidoxime derivatives [9,16,17,25], and **13c** is the most effective SOx reactivator to date (Table 1). We developed and validated molecular models with reactivation improvement (**8c** vs. **8b**, Table 1). SOxs also appear to be relatively non-toxic with guinea pig LD_{50} of 1590 mg kg^{-1} [9]. Assuming a one compartment model, the estimated blood level of SOx at the LD_{50} would be 42 mM. The $LD_{12.5}$ is 10.5 mM and greater than two times the normal Glc blood level of 5 mM. **8b** pharmacokinetics shows that SOx can attain T_{max} quickly (10 min, similar to 2-PAM) from an IM administration but has longer mean residence time (2 h vs. less than 80 min for 2-PAM) [17]. These are all desirable characteristics of a reactivator, but it was the finding of the amelioration of the body temperature depression response to pesticides that made these compounds of interest to cross the BBB [16]. The first experiments to test the transport of **13c** in a BBB model were done with 0.005 and 0.05 mM SOx. No measurable **13c** was found in the receiver wells (Table 2). These experiments, however, were conducted at the typical cellular maintenance Glc concentration of 15–20 mM, so it is possible that at low concentrations **13c** would not compete well for the transporter. We then tested **13c** up to18 mM at the physiologically relevant 5 mM Glc concentration and found that **13c** transport appears to be asymmetric with greater efficiency from the apical (luminal) side. The 18 mM **13c** treatment yielded after 2 h ~7 and 1.7 μM **13c** on the receiver side of apical- and basolateral-treated sides. This sidedness was also apparent for cell lysates with 175 vs. 3.15 μM **13c** found from apical and basolateral dosing respectively. These results indicate that there appears to be significant removal of **13c** from the apical side and nearly none from the basolateral side. We hypothesize that GLUT transporters on the apical side are more efficient than those on the basolatereral side for **13c** such that **13c** becomes trapped inside the cell. In addition, since not all the **13c** mass could be accounted for (~80% unaccounted) which suggests that once inside the cell **13c** is metabolized or catabolized and that the products not are detectable as **13c** (413 *m*/*z*). Further analysis is needed to determine what these might be and whether a functional oxime moiety is transferred across the BBB, though no longer as parent SOx, and explain the apparent CNS effects of SOx; or, there is some other as yet unidentified mechanism for SOx BBB penetration that may not primarily involve GLUTs. Regardless of mechanism, efficacy studies are in order to evaluate the utility of the SOxs.

Attempts at soaking of *Torpedo californica* (*Tc*AChE) crystals with **8b** or **13c** were unsuccessful (data not shown), *Tc*AChE crystals were soaked with various concentrations (5–80 mM) of either **8b** or **13c** SOx. These results demonstrate that SOxs have an apparent low affinity for the apo active *Tc*AChE. The weak molecular interactions are likely the outcome of entropy–enthalpy compensation [26]. A stronger protein–ligand interaction will also result in a reduction of the configurational freedom of the system and thus a reduction of the entropy. Correspondingly, by taking into account effects such as the desolvation enthalpy and entropy and the conformational restriction that accompanies binding, weaker molecular interactions will produce a looser molecular association and an increase in entropy. Studies are in progress to elucidate the structures of VX and GB nonaged and aged conjugated forms of *Tc*AChE with **8b** or **13c**.

The modeling results lay the ground work to examine the molecular dynamics of GLUT-1 transport of SOxs. The docked GLUT-1 molecule and the original PDB molecule 1SUK had an excellent overlay with RMSD values varying from 0.2 to 0.3 Å as shown in Table 6. Table 6 shows that **13c** had lower binding energy values at each location examined than Glc indicating that GLUT-1 would be a relatively poor transporter for **13c**. The ECM2 site had the lowest values for Glc and **13c** and we therefore postulate that the Glc channel has a bottle neck, where the transported molecule is captured with moderate binding affinity of −242 Kcals/mol

for Glc and −582 Kcals/mol for **13c** at the ECM-1; then the molecule translocates to the ECM-2 position and is bound most tightly with binding energy of −477 Kcals/mol for Glc and −868 Kcals/mol for **13c**. After this, the subsequent energies diminish showing that Glc and other Glc-like molecules could traverse through the Glc-channel. The basolateral treatment data supports this finding as there was no apparent facilitated transport from this compartment. In contrast, the different results from the apical treated side suggest that these transporters have some transport potential for the Glc C-1 conjugate as overall transfer is 2× that of the basoloateral side with a 55× greater amount associated with the cell fraction. These results suggest that conjugation through the Glc C-1 site may not be best for facilitated transport by GLUTs. Based on literature reports of drug delivery and the recent GLUT-1 models Glc linked through the C-6 position may produce better compounds for transport. The models we have devised could be applied to these compounds for virtual screening of candidate SOxs.

Conflict of interest statement

None declare.

Acknowledgements

Excellent technical assistance was provided by Ms. Janine Ladzinski for cell culture toxicological testing. This work was supported by Defense Threat Reduction Agency (Grant number 1.E005.08.WR). The views expressed herein are those of the author(s) and do not reflect the official policy of the Department of Army, Department of Defense, or the U.S. Government.

References

[1] E. Shek, T. Higuchi, N. Bodor, Improved delivery through biological membranes. 3. Delivery of *N*-methylpyridinium-2-carbaldoxime chloride through the blood–brain barrier in its dihydropyridine pro-drug form, J. Med. Chem. 19 (1976) 113–117.
[2] B.P. Melchers, I.H. Philippens, O.L. Wolthuis, Efficacy of HI-6 and HLo-7 in preventing incapacitation following nerve agent poisoning, Pharmacol. Biochem. Behav. 49 (1994) 781–788.
[3] G. Cassel, L. Karlsson, L. Waara, K.W. Ang, A. Goransson-Nyberg, Pharmacokinetics and effects of HI 6 in blood and brain of soman-intoxicated rats: a microdialysis study, Eur. J. Pharm. 332 (1997) 43–52.
[4] N.J. Abbott, L. Ronnback, E. Hansson, Astrocyte-endothelial interactions at the blood–brain barrier, Nat. Rev. Neurosci. 7 (2006) 41–53.
[5] J.W. Skovira, J.C. O'Donnell, I. Koplovitz, R.K. Kan, J.H. McDonough, T.-M. Shih, Reactivation of brain acetylcholinesterase by monoisonitrosoacetone increases the therapeutic efficacy against nerve agents in guinea pigs, Chemico-Biol Inter. 187 (2010) 318–324.
[6] J.C. Demar, E.D. Clarkson, R.H. Ratcliffe, A.J. Campbell, S.G. Thangavelu, C.A. Herdman, H. Leader, S.M. Schulz, E. Marek, M.A. Medynets, T.C. Ku, S.A. Evans, F.A. Khan, R.R. Owens, M.P. Nambiar, R.K. Gordon, Pro-2-PAM therapy for central and peripheral cholinesterases, Chemico-Biol. Inter. 187 (2010) 191–198.
[7] B.M. Askew, Oximes and hydroxamic acids as antidotes in anticholinesterase poisoning, Br. J. Pharmacol. 11 (1956) 417–423.
[8] G. Mercey, T. Verdelet, J. Renou, M. Kliachyna, R. Baati, F. Nachon, L. Jean, P.-Y. Renard, Reactivators of acetylcholinesterase inhibited by organophosphorus nerve agents, Acc. Chem. Res. 45 (2012) 756–766.
[9] G.E. Garcia, A.J. Campbell, J. Olson, D. Moorad-Doctor, V.I. Morthole, Novel oximes as blood–brain barrier penetrating cholinesterase reactivators, Chemico-Biol. Inter. 187 (2010) 199–206.
[10] F. Maher, S.J. Vannucci, I.A. Simpson, Glucose transporter proteins in brain, FASEB J. 8 (1994) 1003–1011.
[11] C. Fernandez, O. Nieto, J.A. Fontenla, M.L. Rivas de Ceballos, A. Fernandez-Mayoralas, Synthesis of glycosyl derivatives as dopamine prodrugs: interaction with glucose carrier GLUT-1, Org. Biomol. Chem. 1 (2003) 767–771.
[12] T. Halmos, M. Santarromana, K. Antonakis, D. Scherman, Synthesis of Glc-chlorambucil derivatives and their recognition by the human GLUT-1 Glc transporter, Eur. J. Pharmacol. 318 (1996) 477–484.
[13] G. Masand, K. Hanif, S. Sen, A. Ahsan, S. Maiti, S. Pasha, Synthesis, conformational and pharmacological studies of glycosylated chimeric peptides of Met-enkephalin and FMRFa, Brain Res. Bull. 68 (2006) 329–334.
[14] Y. Huang, M.J. Lemieux, J. Song, M. Auer, D.N. Wang, Structure and mechanism of the glycerol-3-phosphate transporter from *Escherichia coli*, Science 301 (2003) 616–620.
[15] A. Salas-Burgos, P. Iserovich, F. Zuniga, J.C. Vera, J. Fishbarg, Predicting the three-dimensional structure of the human facilitative glucose transporter GLUT-1 by a novel evolutionary homology strategy: insights on the molecular mechanism of substrate migration, and binding sites for glucose and inhibitory molecules, Biophys. J. 87 (2004) 2990–2999.
[16] E. Heldman, Y. Ashani, L. Raveh, E.S. Rachaman, Sugar conjugates of pyridinium aldoximes as antidotes against organophosphonate poisoning, Carbohyd. Res. 151 (1986) 337–347.
[17] J.B. Bhonsle, A.J. Campbell, D. Moorad-Doctor, J. Olson, D. Ghimire, G.E. Garcia. Sugar-oximes as cholinesterase reactivators in the brain, in: Proceedings 27th Army Science Conference, 2010, Orlando, FL.
[18] F. Worek, H. Thiermann, L. Szinicz, P. Eyer, Kinetic analysis of interactions between human acetylcholinesterase, structurally different organophosphorus compounds and oximes, Biochem. Pharmacol. 68 (2004) 2237–2248.
[19] Q. Wang, J.D. Rager, K. Weinstein, P.S. Kardos, G.L. Dobson, J. Li, I.J. Hidalgo, Evaluation of the MDR-MDCK cell line as a permeability screen for the blood–brain barrier, Int. J. Pharm. 288 (2005) 349–359.
[20] N.H. Creasey, A.L. Green, 2-Hydroxyiminomethyl-*N*-methylpyridinium methanesulphonate (PS2), an antidote to organophosphorus poisoning. Its preparation, estimation and stability, J. Pharm. Pharmacol. 11 (1959) 485–490.
[21] K. Inukai, A.M. Shewan, W.S. Pascoe, S. Katayama, D.E. James, Y. Oka, Carboxy terminus of glucose transporter 3 contains an apical membrane targeting domain, Mol. Endocrin. 18 (2004) 339–349.
[22] M. Mueckler, C. Makepeace, Transmembrane segment 6 of the GLUT-1 glucose transporter is an outer helix and contains amino acid side chains essential for transport activity, J. Biol. Chem. 283 (2008) 11550–11555.
[23] P. Cunningham, I. Afzal-Ahmed, R.J. Naftalin, Docking studies show that D-glucose and quercetin slide through the transporter GLUT-1, J. Biol. Chem. 281 (2006) 5797–5803.
[24] J. Holyoake, V. Caulfield, S.A. Baldwin, M.S.P. Sansom, Modeling, docking, and simulation of the major facilitator superfamily, Biophys. J. 91 (2006) L84–L86.
[25] E.S. Rachman, Y. Ashani, H. Leader, I. Granoth, H. Edery, G. Porath, Sugar-oximes, new potential antidotes against organophosphorus poisoning, Arzneim Forsch. Drug Res. 29 (1979) 875–876.
[26] K. Sharp, Entropy–enthalpy compensation: fact or artifact?, Protein Sci 10 (2001) 661–667.
[27] W.L. DeLano. The PyMOL Molecular Graphics System, DeLano Scientific LLC, San Carlos, CA, USA, 2002 <http://www.pymol.org>.